Paper 278

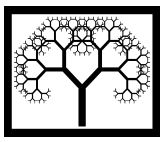

Proceedings of the Eleventh International Conference
on Computational Structures Technology,
B.H.V. Topping, (Editor),
Civil-Comp Press, Stirlingshire, Scotland

Vibration Control of Civil Engineering Structures using Magneto-Rheological Dampers

M.B. Cesar[1] and R.C. Barros[2]
[1] Department of Applied Mechanics
Polytechnic Institute of Bragança (IPB-ESTiG), Portugal
[2] Department of Civil Engineering
Faculty of Engineering of the University of Porto (FEUP), Portugal

Abstract

This paper addresses the semi-active control of a scaled model frame equipped with a magneto-rheological (MR) damper, developed within the COVICOCEPAD project (Eurocores program S3T) reporting related research and development related with structural control of civil engineering structures. The scaled frame is a model of a three-storey building with a single MR damper rigidly connected between the ground and the first floor. Among the variety of semi-active control algorithms available for MR damper control, a clipped-optimal control algorithm model-based on the linear quadratic regulator (LQR) and a fuzzy control non-model-based algorithm were selected as the semi-active controllers. A small sponge type MR damper was experimentally tested under several input excitations to characterize the damper performance. The simple Bouc-Wen phenomenological model was chosen to simulate the nonlinear behavior of the MR damper and the related model parameters were obtained based on the experimentally measured responses. Some numerical results of the uncontrolled and controlled frame under El Centro earthquake are given to evaluate the performance of the selected control strategies.

Keywords: magneto-rheological damper, hysteretic behaviour, semi-active control algorithms.

1 Introduction

Recent developments in civil structures design and construction allowed creating slender and flexible structures such as towers, high-rise buildings and long span bridges. The structural properties of these structures, namely the low damping capability makes them vulnerable to strong wind or earthquake actions [1]. Thus, along with the technological achievements of creating flexible structures arose the necessity to develop devices and additional smart structural systems technologies

(S3T) capable to control the vibrations caused by the external excitations. These control systems can reduce vibrations of these flexible structures to ensure that they respond according with the required functional performance.

In the last decades various control systems based on passive, active, semi-active and hybrid devices have been proposed and different control strategies were developed and implemented for structural vibration control. Among these, the semi-active based control has become an important alternative to passive and active control methods due to its ability to gather some of the advantages of the passive control such as the reliability of these systems with the adaptability of the active control.

MR dampers are semi-active devices that can provide adequate vibration control of civil engineering structures due to their reliability and reduced power requirements. These devices have damping characteristics that can be modified in real time by adjusting the flow of a MR fluid with an applied magnetic field. Changing the properties of the MR fluid allow variations in the damping force that can be controlled by varying an applied current. Thus, a control algorithm that computes the required current level to adjust the MR damper damping force must be employed and several control strategies have been developed and validated for these semi-active devices.

The semi-active clipped-optimal control algorithm was proposed by Dyke *et al.* [2] to reduce the structural response with a MR damper and has become a reference MR damper control approach. This is a model-based algorithm that commands the MR damper operating voltage/current by a linear optimal controller with a force feedback loop. The damping force is compared with the optimal control force and the command signal is selected at either a zero current signal (OFF) or a maximum level current signal (ON). Despite the good results obtained with this controller, its on-off nature, the requirement to measure the damper force and the inability to directly control de damper force lead to the development of more advanced control strategies, namely fuzzy control algorithms.

The semi-active fuzzy control strategy is a robust control method that uses the fuzzy set theory to deal with input uncertainties or disturbances and has the ability to develop a controller without the exact mathematical model of the system. It also has the ability to compute the required current/voltage in order to generate the desirable damper force without measuring the generated damping force [3].

The present research investigates the semi-active control of a small-scale metallic frame equipped with a small MR damper. This frame was designed and assembled within the COVICOCEPAD project (Barros [3]) to study the vibration reduction with several control approaches. Among the several possible control strategies that can be easily used with this scaled frame, Tuned Mass Dampers (TMD), Tuned Liquid Dampers (TLD) and a Base Isolation system (BI) are the more simple to implement due to its passive behaviour [4, 5]. In the present study will be addressed the semi-active control with a MR damper assembled between the ground and the first floor.

To implement a control system it is necessary to choose a numerical model to simulate the non-linear behaviour of the MR damper. The main problem regarding MR damper numerical modelling is the accurate inclusion of the characteristic nonlinear nature of these devices into the model.

Due to the MR effect, this nonlinear behaviour is current and excitation dependent, which increases the difficult task of develop a MR damper model; and also to select an adequate efficient semi-active control strategy.
Among the number of available models, the simple Bouc-Wen model was selected to simulate the MR damper response. This is a parametric model that requires the identification of several model parameters that define the MR damper behaviour. To obtain these parameters it is necessary to have experimental data and afterward initiate an identifying procedure. Then, an experimental program was carried out and the experimental data obtained with this program were later utilized to determine the parameters required to define the simple Bouc-Wen model. An experimental modal identification was also carried out to obtain the dynamic properties of the frame in order to develop a numerical model.
In this study two vibration control approaches were selected to reduce the response of the scaled model frame: the clipped optimal algorithm and a fuzzy theory based control. The purpose of using these two control strategies is to compare their performance and efficiency to control the vibration induced by a simulated earthquake signal. A numerical model of the system was developed and one of the ElCentro records was used as the earthquake input signal. The performance of the two control systems is then compared with the results of similar response parameters of the uncontrolled structure and of several passive configurations of the MR damper.

2 Experimental Setup

2.1 Scaled metallic frame model

According with the research program of the COVICOCEPAD Eurocores S3T project, the structural setup was developed to study the dynamic behaviour of a 3-d.o.f. scaled metallic frame with semi-active devices [6]. The experimental scaled building is a single bay three-storey frame in shear frame configuration, with the columns at the corners having the same stiffness as shown in Figure 1.
The sponge MR damper was placed horizontally at the first floor level attached to the frame and rigidly connected to the ground (shaking table) as shown in Figure 2. To measure the damping force generated during the experimental tests a load cell is placed in the MR damper support system.
An impulse hammer test was carried out in order to characterize the dynamic properties (natural frequencies, damping and modal participation factors) of the structure in response to an applied excitation. The main purpose was to obtain the Frequency Response Functions (FRF) of the experimental frame (Cesar and Barros [6, 7]). The dynamic parameters of the scaled frame were then obtained based on the data provided by these functions and are tabulated in Table 1. These data were used to develop the numerical simulation model.

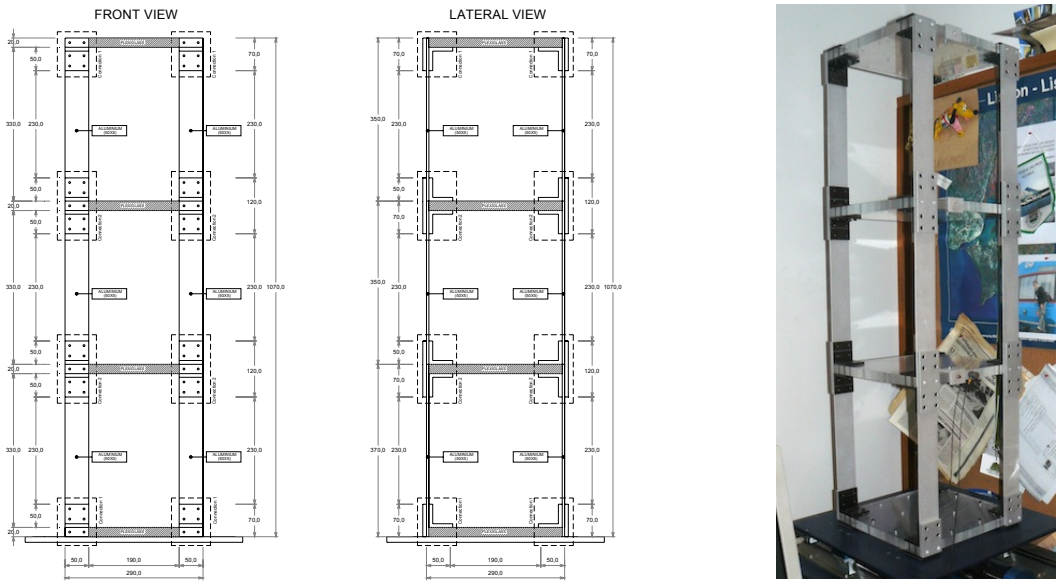

Figure 1. Scaled frame model of a 3-dof system (FEUP-Covicocepad project).

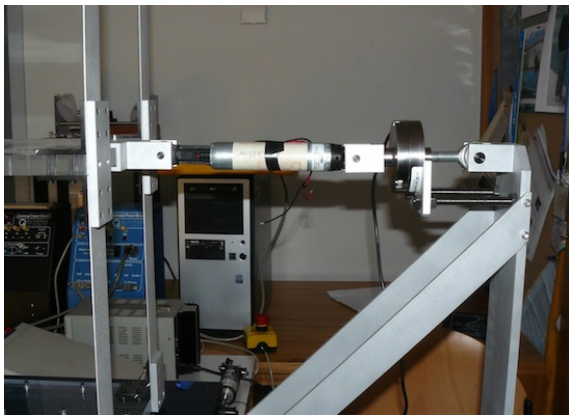

Figure 2. MR damper attached to the first floor of the experimental metallic frame.

	Frequency	Damping	Modal Participation
Mode 1	1,913986	0,03157	34,43248
Mode 2	5,627778	0,01198	35,25975
Mode 3	8,086245	0,00899	30,30777

Table 1 – Parameters of the scaled frames

2.2 MR damper experimental tests

To study the behaviour of a MR damper some experiments were carried out on a MTS universal testing machine (of the Mechanical Engineering Laboratory at FEUP) with the MR damper device RD-1097-1 shown in Figure 3. This is a small

sponge type MR damper with a conventional cylindrical body configuration and an absorbent matrix saturated with an MR fluid in the piston rod. The enclosing cylinder is 32.0 mm in diameter and the damper is 253 mm long in its extended position with ±2.5 cm stroke. The device can operate within a current range from 0.0 A up to 1.0 A with a recommended input value of 0.5 A for continuous operation and can deliver a peak force of 100 N at a velocity of 51 mm/s with a continuous operating current level of 1.0 A. Thus, this damper can be used to control experimental models of structural systems requiring small control forces.

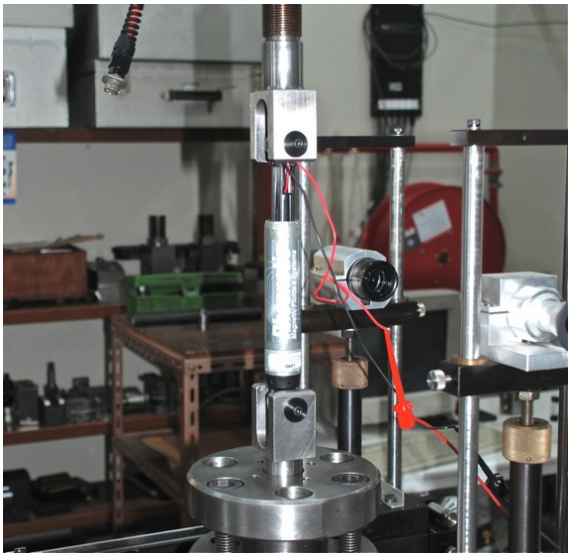

Figure 3: RD-1097-1 MR damper connected to the MTS testing machine.

A parametric study was carried out for several combinations of amplitudes, frequencies and input currents, in order to obtain the required data to characterize the damper response and further develop a numerical model based on the experimental data. Hence, the damper was subjected to a series of predefined sinusoidal displacement excitations through a MTS actuator system working in displacement control mode.
The excitation signals were automatically generated with the MTS controller and a regulated power supply unit was used to provide the constant current supply for each set of sinusoidal signals. The selected set of frequencies, amplitudes and current supplies involved in the experimental procedure are detailed in Table 2.

Parameter	**Values**
Frequencies (Hz)	(0.50, 1.00, 2.00)
Amplitudes (mm)	(2.5, 5.0, 7.5)
Current supplies (A)	(0.00, 0.10, 0.20, 0.30, 0.40, 0.50)

Table 2 - Parameter variation for the MR damper experimental analysis

The testing procedure was carried out with a fixed frequency and a fixed amplitude sinusoidal displacement for a specific current supply, repeating this process for every parameter combination. The experimental data of the parametric study were grouped into frequency-dependent tests, amplitude-dependent tests and variable input current tests. The responses of the MR damper for the variable input current tests are shown in Figure 4. In this case, the MR damper response was obtained varying the input current while the amplitude and frequency are kept constant.

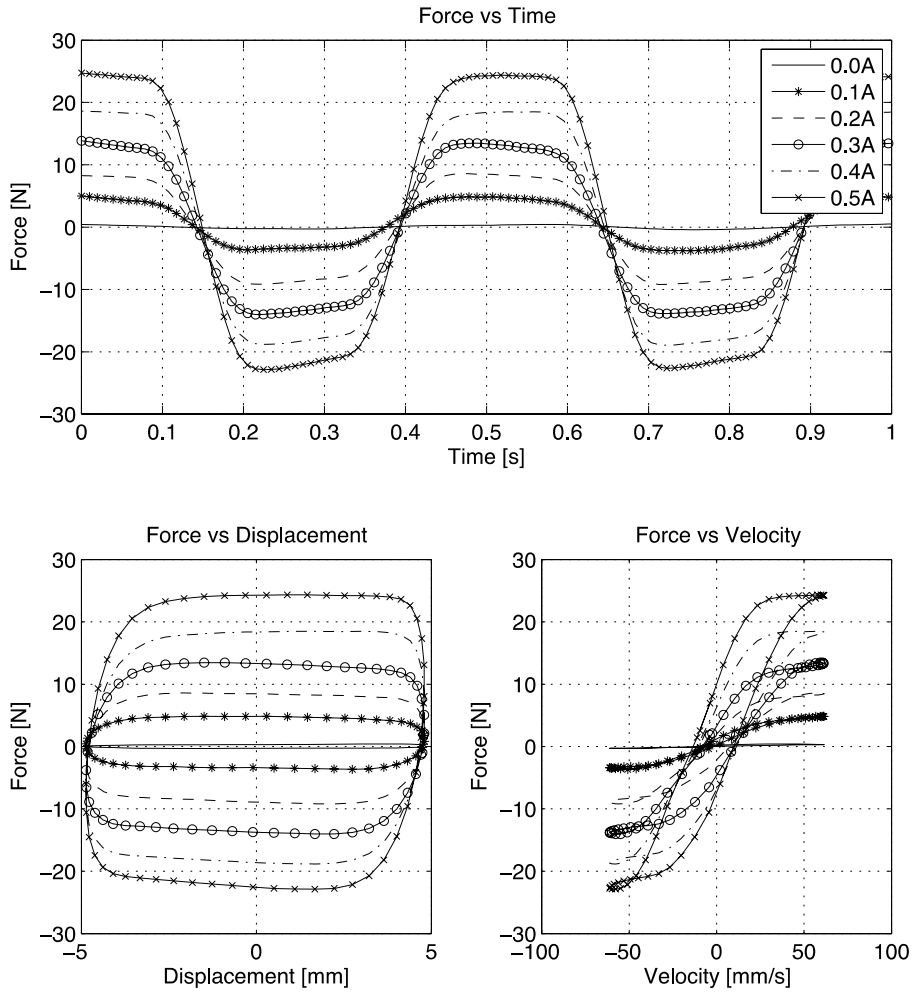

sinusoidal excitation with amplitude of 5.00 mm and variable input current.

Different constant current levels were selected according with the values referred in Table 2 and different amplitudes and frequencies were applied for each current level. The maximum input current level was set to 0.5A and a thermocouple was used to monitor the damper temperature to avoid overheating that could damage the device.
As expected, the damping force increases with the input current level and the hysteretic behaviour is also intensified. When the device is operating without input current, the damper response reveals a reduced hysteretic loop; while operating with

a non-zero constant input current level, the damper exhibits a significantly larger hysteretic behaviour.
An increase in the input current means that the magnetic field to which the MR fluid is exposed is also increasing and therefore the mechanical properties of the fluid are changed, specially the yield force that causes a plastic-like behaviour in the hysteresis loops. In the post-yield region it is perceptible that the rate of change of the damping force with respect to the velocity is moderately low while the damper presents substantial hysteresis characteristics in the pre-yield operation regime.

3 Semi-Active Control

To develop a control system with MR dampers it is necessary to select a control algorithm that efficiently uses the MR damper to reduce the structural response of the system that is been controlled. The MR damper is capable of generating a damping force according with an input current/voltage. Thus, the control strategy is selected so that the generated damping force can track a desired command damping force.
In the last few years several approaches have been proposed and intensively studied for better selection of the input current/voltage that must be applied to the MR damper to efficiently achieve a desired performance. In this study, the clipped-optimal control and a fuzzy based control were selected as the semi-active control methods to command the MR damper.

3.1 Clipped-optimal control

Dyke *et al.* [2] proposed the clipped optimal control system shown in Figure 5. This approach has proved to be a good strategy to implement semi-active MR devices in civil engineering structures.

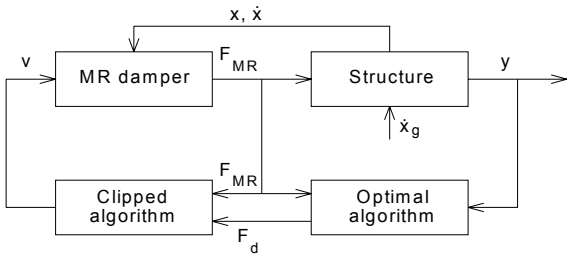

Figure 5: Semi-active clipped optimal control system.

This controller drives the damper to generate a desirable control force determined by an “ideal” active controller. A force feedback is used to produce the desired control force f_d, which is determined by a linear optimal controller $K_k(s)$, based on the measured structural responses y and the measured damper force f_c. Only applied voltage v_a can be commanded and not the damper force. The algorithm for selecting such voltage is

$$v_a = v_{\max} H\left(f_d - f_c\right) f_c \tag{1}$$

in which v_{max} is the voltage level associated with the saturation of the magnetic field in the MR damper and H is the Heaviside step operator. The following voltage selection algorithm is applied: When the actual force being generated by the damper f_c equals the desirable force f_d, the voltage applied remains the same; when the magnitude of the force f_c is smaller than the magnitude of f_d and both forces have the same sign, then the voltage applied is set to its maximum level to increase the damper force; otherwise, voltage is set to zero.
This algorithm is given by

$$f_{MR} = \begin{cases} f_d, & f_d \cdot \dot{x} < 0 \\ 0, & \text{otherwise} \end{cases} \tag{2}$$

where f_{MR} is the MR damper control force. According with this algorithm, the control forces that are outside the MR damper range are clipped in a bang-bang controller. Thus, the command signal is set at zero or at the maximum level depending on the comparison between the force being generated by the damper and the desirable force.
The selected optimal controller is based on a Linear Quadratic Optimal Control. In this numerical study the linear controller is obtained with a Linear Quadratic Regulator (LQR) strategy that is used in a state feedback control.
The main objective to design the optimal controller is to obtain an optimal control vector $f_c(t)$ that minimizes a performance index J. In this case a quadratic performance index in $z(t)$ and $f_c(t)$ is used and is represented by:

$$J = \int_0^{t_f} \left[z^T(t) \cdot Q \cdot (t) + f(t) \cdot R \cdot f(t) \right] dt \tag{3}$$

In this equation Q and R are weighting matrices associated with the state variables and with the input variables respectively. The magnitudes of these matrices are defined according with the importance that is given to the state variables and the control forces on the minimization process. Increasing the values of Q matrix elements implies to prioritize the response reduction over the control forces. By other hand, increasing the values of the elements of R implies to prioritize the control forces rather than the response reduction.
The solution of the LQR problem is based on the analysis of the algebraic Riccati equation

$$PA + A^T P - PBR^{-1} B^T P + Q = 0 \tag{4}$$

and the LQR problem can be solved using a linear state feedback with a constant gain G according with

$$u(t) = -G \cdot x(t) = \left[R^{-1} B^T P \right] \cdot x(t) \tag{5}$$

To select the appropriate values for Q and R the following procedure was used in this study [7]: it was assumed that R matrix has the following form

$$R = r \cdot I \tag{6}$$

where I is the identity matrix and r is a multiplier, and that Q matrix assume the following form

$$Q = \begin{bmatrix} K & 0 \\ 0 & 0 \end{bmatrix} \tag{7}$$

A parametric study must be carried out to select the value of the multiplier to verify the efficiency of the control (reduction of floor displacements, accelerations and also the control force on the actuator).

3.2 Fuzzy control

The fuzzy control is an intelligent control system based on fuzzy logic that essentially involves three basic components: fuzzification, fuzzy inference and defuzzification. A schematic representation of the fuzzy control components is shown in Figure 6.

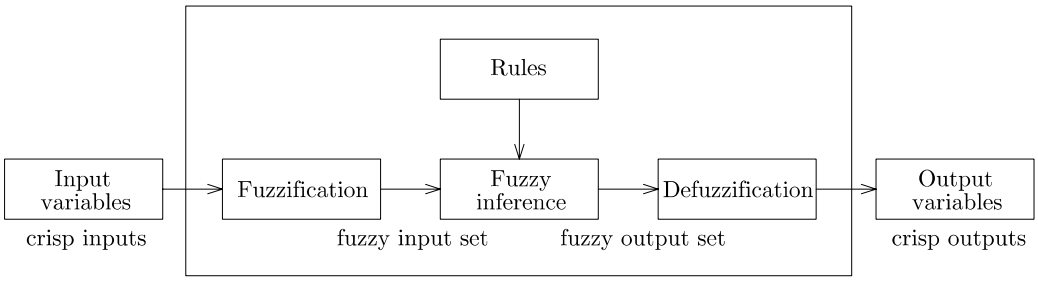

Figure 6: The fuzzy control inference algorithm.

The fuzzification is the process of transforming crisp values (input variables) into grades of membership for linguistic terms of fuzzy sets. For each input and output variable some membership functions with a qualitative category such as low, normal or high are defined. The shape of these functions can be selected according with the distribution of the crisp set and the original data can be fuzzified based on Gaussian, triangular, trapezoidal or other membership functions. Fuzzy rule inference is the process where the rule inference (fuzzy IF–THEN-ELSE rules) is computed. Essentially, the procedure uses fuzzy set theory to map inputs to outputs. Finally, the defuzzification process is employed to ensure that the control variables are

determined by the system. In this phase, the fuzzy outputs are converted into a scalar and physically interpretable output quantities. Several defuzzification methods are available and the Centroid Defuzzification Technique (center of gravity or center of defuzzification area) is the most commonly used technique. This defuzzification technique can be expressed as follows [4]

$$y_j = \frac{\sum_{l=1}^{N} B_l^j \left[\Pi_{i=1}^{p} \mu_{A_i^j}(x_i) \right]}{\sum_{l=1}^{N} \left[\Pi_{i=1}^{p} \mu_{A_i^j}(x_i) \right]} \tag{8}$$

where x_i are the inputs of the fuzzy controller and A_i^j is the linguistic value with respect to x_i of rule j. The outputs of the fuzzy controller are given by y_i and B_l^j is a fuzzy singleton function. Finally, μ_A is the membership function of A_i^j.

4 Numerical Analysis

To study the response of the semi-active control of the scaled 3-d.o.f. frame model with the selected semi-active controllers, a numerical analysis was carried out. A state space formulation was used to develop the control system and one of the El Centro records was used as the earthquake input signal.

Before developing the numerical analysis it is necessary to construct a numerical model of the MR damper. The accuracy of the model becomes a very important factor to successfully achieve desirable control performance in order to easily integrate the device into a control system. Parametric models are a common approach to simulate the behaviour of MR dampers. In this case the MR damper is characterized by a system of mechanical elements with linear or non-linear behaviour including springs, dashpots and other elements in order to obtain a mathematical model that correctly incorporate the nonlinear behaviour of these devices. Among these parametric models, the Bouc–Wen hysteresis model is one of the most widely accepted approaches to simulate an extensive variety of hysteretic behaviour. In the present study a simple Bouc-Wen model was selected to simulate the dynamic response of the RD-1097-1 sponge MR damper. The model parameters of the Bouc-Wen model were obtained based on the experimental tests presented earlier in this paper.

A numerical routine was developed and two control strategies were adopted: a clipped-optimal control and a fuzzy control. To implement the clipped-optimal control it is necessary to study the influence of the weighting matrices Q and R while the fuzzy control requires the definition of the distribution and type of the membership functions. In the present section will be presented the weighting matrices and membership functions used to perform the numerical analysis of the scaled model frame. Finally, the numerical performance of each strategy is then compared with the uncontrolled and passive configuration of the scaled model.

4.1 Bouc-Wen model

The model was introduced by Bouc [8] and later generalized by Wen [9] who demonstrated the versatility of this model to represent a large variety of hysteretic patterns. Due to this advantageous characteristic, the model was used to describe several nonlinear hysteretic systems such as hysteretic isolators and MR dampers.
Although MR dampers exhibit a well-defined typical behaviour, the final hysteretic configuration depends on some particular behavioural features related with the damper geometry, presence of an accumulator, etc. Therefore, the model must be adapted to include the realistic MR damper behaviour and several variations of the Bouc-wen model were developed to correctly simulate MR dampers.
Among these models, the simple Bouc-Wen model will be used to simulate the hysteretic response of a MR damper. The simple Bouc-Wen model has three components: a spring, a dashpot and a Bouc-Wen block, in a parallel configuration as shown in Figure 7. The non-linearity of the system is located in the Bouc-Wen block, which is capable to capture the behaviour of MR dampers.

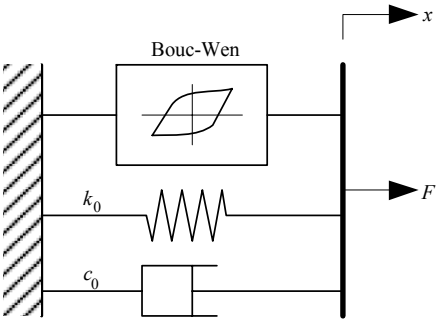

Figure 7: Simple Bouc–Wen model [10].

This model was adopted by Spencer *et al.* [10] to study the behaviour of a MR damper comparing the performance of this model with other parametric models. The damping force in this system is given by

$$F(t) = c_0\dot{x} + k_0(x - x_0) + \alpha z \tag{9}$$

where c_0 is the viscous coefficient, k_0 the stiffness coefficient and z is an evolutionary variable associated with the Bouc-Wen block and governed by

$$\dot{z} = -\gamma \mid \dot{x} \mid z \mid z \mid^{n-1} -\beta\dot{x} \mid z \mid^{n} +A\dot{x} \tag{10}$$

The initial displacement x_0 allow including the presence of an accumulator into the system. The parameters c_0, k_0, α, β, γ, n and A are usually called characteristic or shape parameters of the Bouc–Wen model and are functions of the current applied to the MR damper, the amplitude and frequency of vibration. The non-linear shape of the hysteretic curve can be adjusted by changing the values of the Bouc-Wen block

parameters allowing to control the linearity in the unloading and the smoothness of the transition from the pre-yield to the post-yield region.
The sponge-type MR damper presents a well-defined hysteretic behaviour that can be easily simulated by the Bouc-Wen model. The device produces a smooth hysteretic loop and since it does not have an accumulator, the distinctive loading/unloading force oscillations caused by the accumulator are not present. Then, a precise hysteretic numerical response is expected.
A set of constrains for each model parameter were selected and implemented in the identification algorithm to accelerate the minimization procedure. The parameter n=1 was defined according with the results obtained in previous research work [11] and finally, the force offset $f_0 \approx 0$.
Usually, the parameter identification approach consists of formulating an optimization problem to find the best match between the experimental data and the dynamic model representation. A schematic representation of the optimization procedure that can be used to estimate the model parameters of MR damper dynamic models is shown in Figure 8 [12].

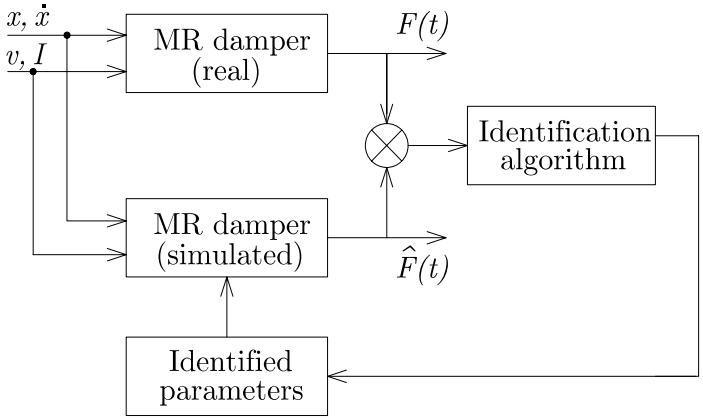

Figure 8: Parameters identification for MR dampers.

Figure 9 illustrates the result of the parameter identification for the Bouc-Wen model when the damper is driven with a sinusoidal excitation of 1.00 Hz with 5mm amplitude and an operating current of 0.50A. The identification procedure was repeated for each set of experimental data and the different values of the model parameters of the Bouc-Wen model were determined.
The parameters current independent A, β, γ are considered as constant values during the sinusoidal excitation and the average values A= 38.012, β=-1.401 mm^{-2}, γ=4.794 mm^{-2} and k_0 = 0.01 N/mm were estimated. The polynomial functions of the current/voltage dependent parameters α, and c_0 were obtained with a polynomial curve fitting as shown in Figures 10 and 11 respectively. These parameters can be described by polynomial function as

$$\alpha(I) = -9.66I^3 + 9.76I^2 + 1.12I + 0.10 \tag{11}$$

$$c_0(I) = 4.48I^4 - 4.74I^3 + 1.35I^2 + 0.05I + 0.01 \tag{12}$$

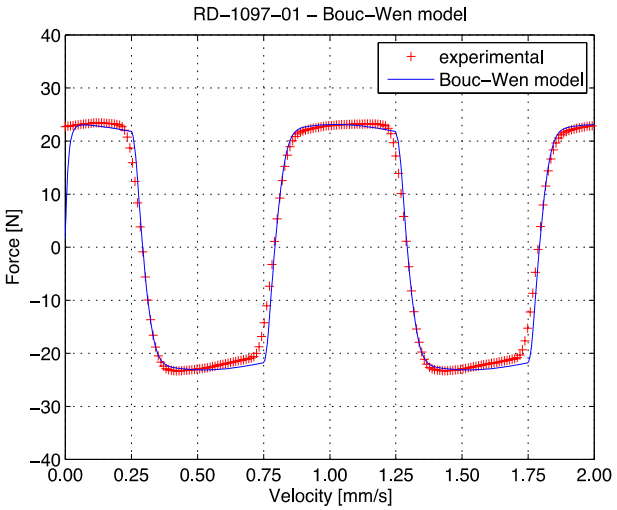

Figure 9: RD-1097-1 MR damper – Parameter identification of the Bouc-Wen model under 1.50 Hz sinusoidal excitation with 5mm amplitude and 0.50A.

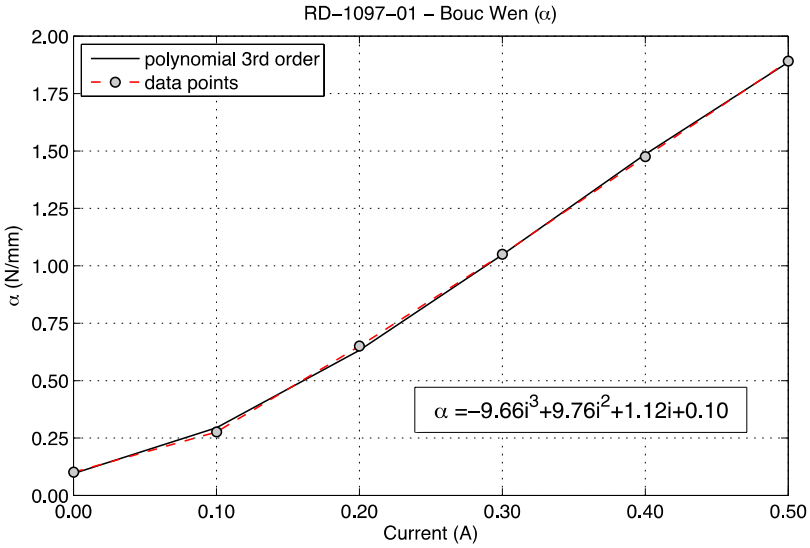

Figure 10: Curve fitting for parameter $\alpha(I)$ of the Bouc-Wen model.

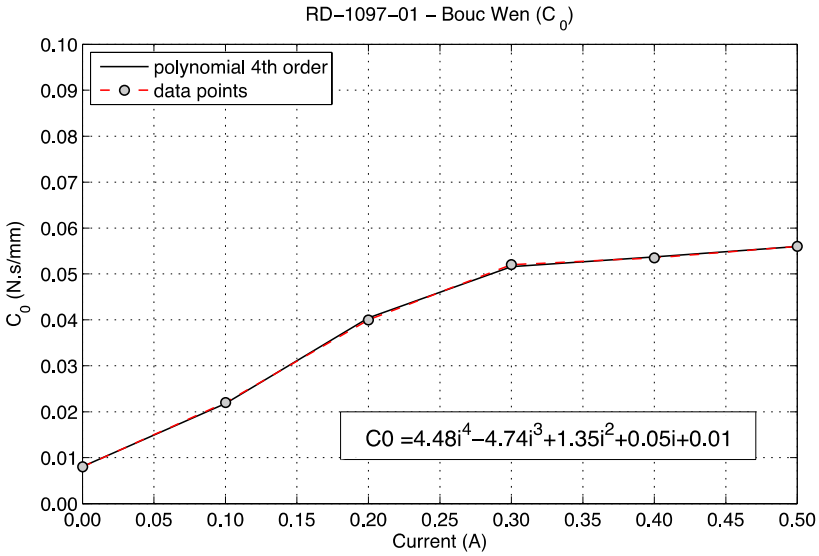

Figure 11: Curve fitting for parameter $c_0(I)$ of the Bouc-Wen model.

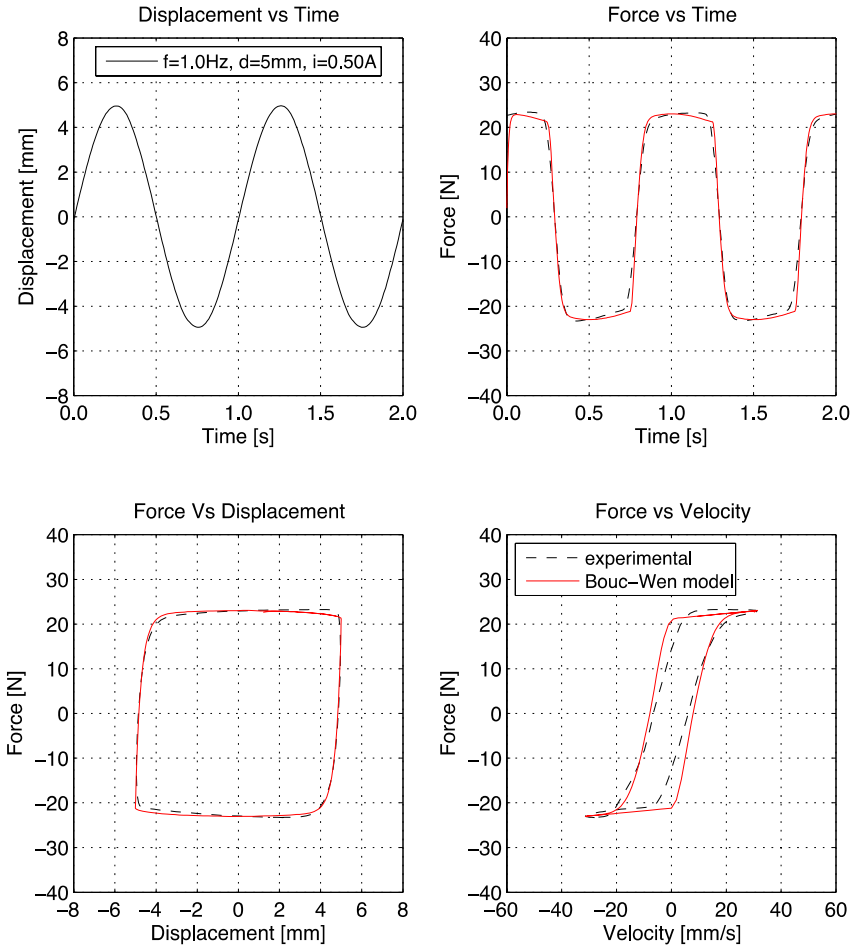

Fig he Bouc-Wen model (1.50 Hz sinusoidal excitation with 5mm amplitude and 0.50A).

Figure 12 illustrates the numerical and experimental responses for a sinusoidal excitation with 1.00 Hz frequency, 5mm amplitude and 0.50A.

4.2 Semi-active control formulation

The equation of motion that describes the behaviour of a controlled building under an earthquake load, Barros *et al.* [13] Cesar and Barros [14-15], is given by:

$$M\ddot{x} + C\dot{x} + Kx = -\Gamma f - M\lambda\ddot{x}_g \tag{13}$$

where M is the mass matrix, C is the damping matrix, K is the stiffness matrix, x is the vector of floors displacements, $\dot{x}$ and $\ddot{x}$ are the floor velocity and the acceleration vectors respectively, f is the measured control force, λ is a vector of ones and Γ is a vector that accounts for the position of the MR damper in the structure.
This equation can be rewritten in the state-space form as

$$\dot{z} = Az + Bf + E\ddot{x}_g \tag{14}$$

$$y = Cz + Df + v \tag{15}$$

where z is the state vector, y is the vector of measured outputs and v is the measurement noise vector. The other matrix quantities are defined by

$$\begin{aligned} A &= \begin{bmatrix} 0 & I \\ -M^{-1}K & -M^{-1}C \end{bmatrix} \qquad B = \begin{bmatrix} 0 \\ M^{-1}\Gamma \end{bmatrix} \quad E = -\begin{bmatrix} 0 \\ \lambda \end{bmatrix} \\ C &= \begin{bmatrix} -M^{-1}K & -M^{-1}C \\ I & 0 \end{bmatrix} \qquad D = \begin{bmatrix} M^{-1}\Gamma \\ 0 \end{bmatrix} \end{aligned} \tag{16}$$

The mass, stiffness and damping of the structure are required. According with the dynamic properties of the 3-d.o.f. scaled frame, the mass of each floor is m=3.65 kg, the stiffness is k=2950 N/m and the damping matrix was chosen as $C=0.05\ M$.
The clipped optimal algorithm was the first control strategy to be studied based on employing a linear quadratic regulator (LQR) algorithm with full state feedback (in this numerical analysis). Hence for designing a LQR controller, the aim is to minimize the cost function with appropriate weighting matrices Q and R whose magnitudes are assigned according to the relative importance attached to the state variables and the control forces in minimization procedure. The Q matrix was kept constant and a parametric study was carried out to select the value of the multiplier r related with the R matrix. It was verified that decreasing this value implies a more evident reduction response and in this case a significant reduction of the floor displacements and accelerations was obtained with $r=10^{-15}$.
The design of a fuzzy logic-based controller comprises the selection of the input variables, the distribution and type of membership functions and finally the output

variables that are required to generate the control command signal. One of the fundamental issues in fuzzy sets is how to define the fuzzy membership functions. There are different shapes of membership functions and in this case a triangular shape was chosen for the input and output variables as shown in Figure 13.

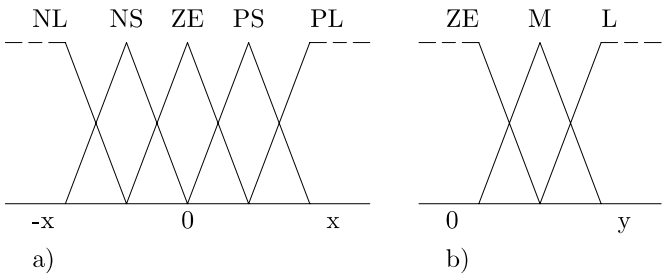

Figure 13: Fuzzy controller input and output membership functions:
a) Input membership function. b) Output membership function.

The controller is designed based on the velocity of the first and third floor [3]. Thus, the controller has two input variables defined by the first-floor velocity and the third-floor velocity. Each variable is defined by five input membership functions with the following fuzzy variables: NL=negative large, NS=negative small, ZE=zero, PS=positive small, and PL= positive large. The output variable represents the command current and is defined by three membership functions with the following fuzzy variables: ZE=Zero, M=medium and L=large.
Before applying the fuzzy logic, the input values are normalized with respect to the maximum velocity value obtained in the uncontrolled configuration. This ensures that the inputs are within the range of the membership functions. The output is normalized and a multiplier is used to obtain a valid command current value.
The fuzzy inference rule shown in Table 3 was determined considering that when both first and third floor velocities (inputs) are very large the command current (output) is large while for small velocities the command current is medium.

	NL	**NS**	**ZE**	**PS**	**PL**
NL	L	L	M	L	M
NS	L	M	ZE	M	ZE
ZE	M	ZE	M	ZE	M
PS	ZE	M	ZE	M	L
PL	M	L	M	L	L

Table 3 – Fuzzy inference rule.

4.3 Numerical results

For the numerical results presented herein, the N-S component of the 1940 El Centro earthquake record (Imperial Valley Irrigation District Station) shown in Figure 14 was chosen as the ground excitation (after being scaled to a PGA of 1 m/s^2).

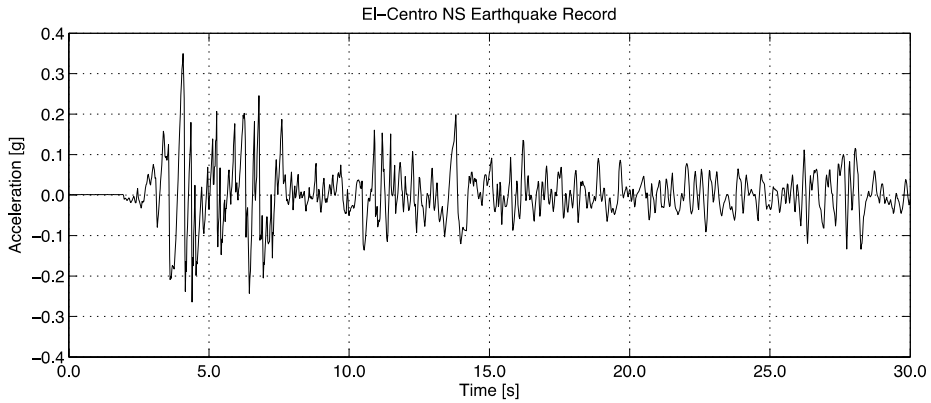

Figure 14: El Centro N-S earthquake record.

The horizontal floor displacement was selected as the reference parameter to verify the efficiency of the control law for the El Centro earthquake signal. The first case to be studied is the response of the uncontrolled system. The resulting floor displacements without a MR damper attached to the frame are shown in Figure 15.

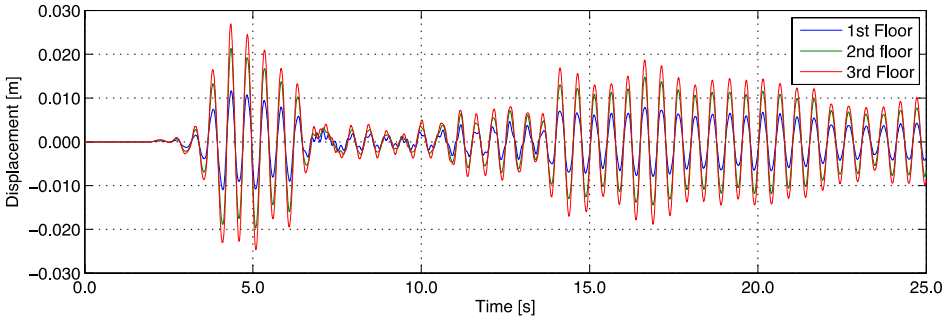

Figure 15: El Centro - Uncontrolled response (floor displacements).

Then, the MR damper was attached to the 1st floor in a passive-off configuration (0.0A) and the floor displacements plot shown in Figure 16 was obtained. The insertion of the MR damper produced a small floor displacement reduction.

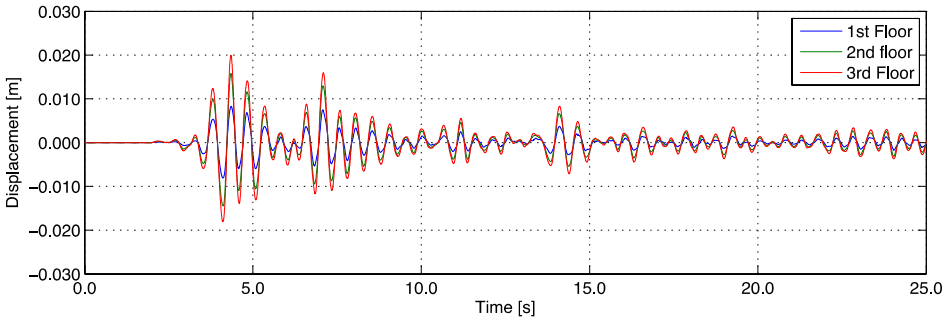

Figure 16: El Centro-Uncontrolled response with MR damper @0.0A.

For the passive-on cases, the MR damper was fed with a constant current of 0.10A, and 0.40A. Figure 17 present the structural response for the first passive-on case (0.10A). In this case the first floor displacement was considerably reduced because the MR damper adds a partial constraint at the first floor level.

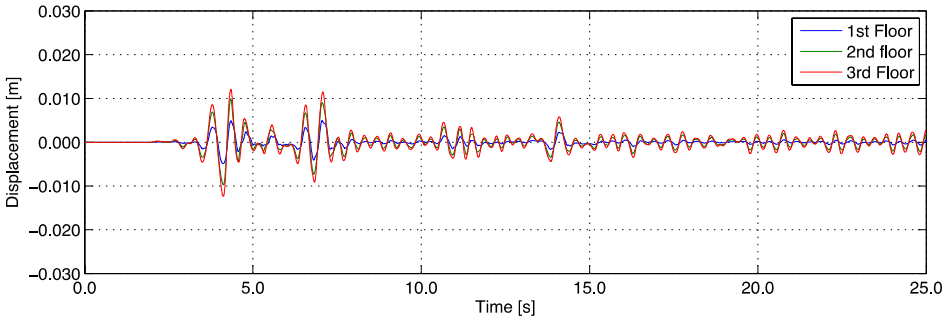

Figure 17: El Centro-Uncontrolled response with MR damper @0.10A.

Figures 18 represent the structural response for constant current of 0.40A. The constraint effect is increased with the increase of the operating current. When the current is at the maximum value, the frame performs like a 2 DOF system above the first floor level. Therefore, the maximum command current of the semi-active configuration should remain under 0.40A.

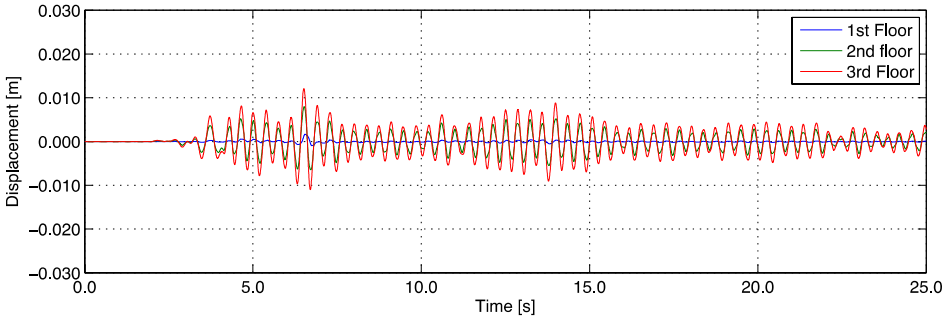

Figure 18: El Centro-Uncontrolled response with MR damper @0.40A.

The MR damper was driven with the command current produced by the clipped-optimal algorithm. Figure 19 shows the floor displacements obtained with this semi-active controller.

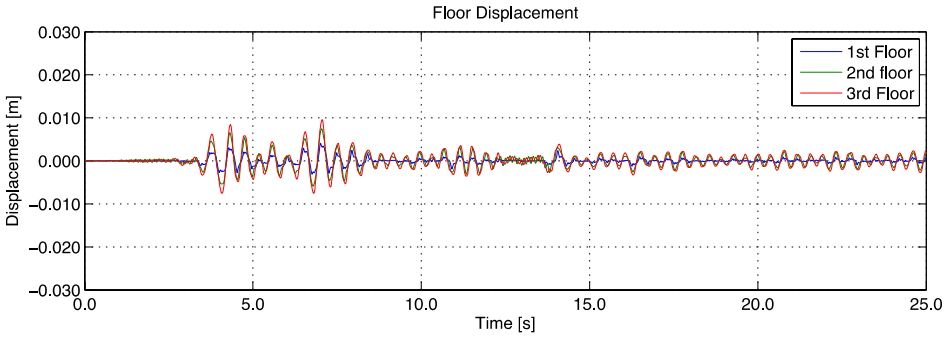

Figure 19. El Centro-Controlled response with MR damper (Clipped optimal).

The results of the Clipped Optimal algorithm reveal that this control strategy is capable to reduce the floor displacements during the earthquake duration.
Finally, the fuzzy controller was applied and the resulting floor displacements are shown in Figure 20.

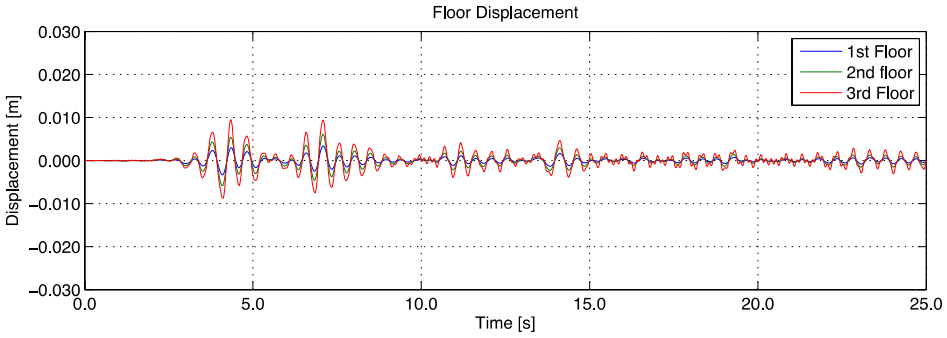

Figure 20. El Centro-Controlled response with MR damper (Fuzzy control).

As seen in this figure, the fuzzy based controller is also capable to effectively reduce the structural response. To compare the performance of the two controllers to reduce the structural response, the maximum displacement and acceleration and the response reduction for each control case with respect to the uncontrolled case are summarized in Table 4.
As expected, the fuzzy based control and the clipped optimal control are able to reduce the structural response of the scaled frame. Although these two control strategies have comparable performances, the fuzzy controller shows a slightly better overall performance than the clipped optimal controller since it is capable to reduce both floor displacements and accelerations.
In the passive-off case the MR damper is used without operating current, allowing a reduction to 70-76% of the uncontrolled floor displacements and accelerations.
The first passive-on case (0.10A) decreases the displacement up to 42-44% and the accelerations up to 55-60% compared with the uncontrolled case while the second passive-on case (0.40A) essentially produce substantial reduction of the first floor displacement (to 15% of the uncontrolled case) due to the constraint effect that create a 2dof response above the first floor.

Control case		Disp. (m)	Reduction (%)	Acc. (m/s^2)	Reduction (%)
Uncontrolled	1st	0.01160	-	2.536	-
	2nd	0.02131	-	4.052	-
	3rd	0.02697	-	5.142	-
Passive-off	1st	0.00832	71,7	1.792	70,7
	2nd	0.01559	73,1	3.080	76,0
	3rd	0.01986	73,6	3.698	71,9
Passive-on (0.1A)	1st	0.00487	42,0	1.513	59,7
	2nd	0.00992	46,6	2.244	55,4
	3rd	0.01198	44,4	3.103	60,3
Passive-on (0.4A)	1st	0.00168	14,5	0.838	33,0
	2nd	0.00793	37,2	2.242	55,3
	3rd	0.01207	44,8	3.616	70,3
Clipped-optimal	1st	0.00384	33,1	1.831	72,2
	2nd	0.00713	33,5	1.843	45,5
	3rd	0.00956	35,4	3.354	65,2
Fuzzy control	1st	0.00338	29,1	1.124	44,3
	2nd	0.00676	31,7	1.572	38,8
	3rd	0.00958	35,5	3.108	60,4

Table 4 – Peak responses under the N-S El Centro earthquake record (PGA=1 m/s^2).

The maximum peak responses in the clipped optimal controller are significantly reduced compared with the uncontrolled case: about 33% of uncontrolled floor displacements and 72%, 46% and 65% of the uncontrolled floor accelerations.
The fuzzy controller has almost the same performance as the clipped optimal controlled regarding the floor displacement reduction but it is more efficient to control the floor accelerations.

5 Conclusions

The present paper addressed the performance of two vibration controllers to reduce the structural response of a scaled three degree of freedom frame equipped with a sponge type MR damper device. The research was developed based on the properties of an experimental frame that was designed within the COVICOCEPAD Eurocores S3T project. Some basic experimental testing results are presented in order to obtain the dynamic response of this structural system. A sponge type MR damper was used to control the structural response of the scaled frame. This damper was experimentally tested to find its rheological response and a parametric model was developed to simulate its behaviour. The model parameters of the numerical model were obtained based on the experimental data. A numerical analysis was carried out based on the dynamic properties of the experimental frame to study the efficiency of a MR damper placed on the first floor to control the responses of the three-story frame. The numerical results show that both control algorithms are capable of

reducing the structural response resulting in a very significant improvement over the uncontrolled system.

Acknowledgements

The authors gratefully acknowledge the previous funding until December 2010 of the S3T Eurocores project COVICOCEPAD, and the funding of the first author by *Ministério da Ciência, Tecnologia e Ensino Superior*, FCT, Portugal, under grant SFRH/BD/49094/2008.

References

[1] B.F. Azar, N.M. Rahbari and S. Talatahari, "Seismic Mitigation of Tall Buildings using Magneto-Rheological Dampers", Asian Journal of Civil Engineering (Building and Housing), Vol. 12, No. 5, pp 637-649, 2011.

[2] S.J. Dyke, B.F. Spencer, M.K. Sain, J.D. Carlson. Modeling and control of magnetorheological dampers for seismic response reduction. Smart Materials and Structures, Vol. 5, pp. 565–575, 1996.

[3] R.C. Barros, "Project COVICOCEPAD under Smart Structural Systems Technologies of Program Eurocores"; World Forum on Smart Materials and Smart Structures Technologies (SMSST-2007), Smart Materials and Smart Structures Technology, Taylor & Francis Ltd, 2008.

[4] C. Kang-Min, C. Sang-Won, J. Hyung-Jo, L. In-Won, "Semi-Active Fuzzy Control for Seismic Response Reduction using Magneto-Rheological Dampers", *Earthquake Engineering and Structural Dynamics*, Vol. 33, pp. 723-736, John Wiley & Sons, Ltd., 2004.

[5] R.C. Barros, A. Baratta, O. Corbi, M.B. Cesar, M.M. Paredes, "Some Research on Control of Vibrations in Civil Engineering under COVICOCEPAD Project", *Third International Conference on Integrity Reliability & Failure* (IRF 2009), 2009.

[6] M.B. Cesar, R.C. Barros, "Semi-Active Control of a Metallic Scaled Frame with a MR Damper: Numerical and Experimental Research", School and Symposium on Smart Structural System Technologies, Editors: R.C. Barros and A. Preumont, FEUP – Porto, pp. 419-440, 2010.

[7] M.T. Braz-Cesar, R.C. Barros, "Semi-Active Control of an Experimental Frame using MR Dampers: numerical results and experimental validation", COMPDYN 2011 – 3rd International Conference on Computational Methods in Structural Dynamics & Earthquake Engineering, 2011.

[8] R. Bouc, "Forced vibration of mechanical systems with hysteresis", Proceedings of the Fourth Conference on Nonlinear Oscillation, pp. 315, 1967.

[9] Y.K. Wen, "Method for random vibration of hysteretic systems", Journal of the Engineering Mechanics Division, 102-2, 249-263, 1976.

[10] B.F. Spencer Jr., S.J. Dyke, M.K. Sain, J.D. Carlson, "Phenomenological model of a magnetorheological damper", Journal of Engineering Mechanics, 123, 230-238, 1997.

[11] Y. Shen, M.F. Golnaraghi, G.R. Heppler, "Load-Leving suspension system with a magnetorheological damper", *Vehicle System Dynamics*, Vol. 45, Issue 4, pp. 297-312, 2007.
[12] D.H. Wang, W.H. Liao, "Magnetorheological fluid dampers: a review of parametric modelling", Smart Materials and Structures, 20, 023001, 2011.
[13] R.C. Barros, R. Bairrão, F. Branco, I. Corbi, M. Kemppinen, G. Magonette, F. Paulet, G. Serino, "Implementation of Structural Control", International Journal of Earthquake Engineering and Engineering Seismology, European Earthquake Engineering 2.05, Vol. XIX-2, pp. 51-68, Patròn Editore, 2005.
[14] M. Braz-César, R. Barros, "Semi-active Vibration Control of Buildings using MR Dampers: Numerical and Experimental Verification", 14th ECEE – 14th European Conference on Earthquake Engineering, 2010.
[15] M. Cesar, R. Barros, "Semi-Active Vibration Control of a 3-DOF Scaled Frame with a Magneto-Rheological Damper", CST2010 – The Tenth International Conference on Computational Structures Technology, 2010.